Cooling capacity and acoustic performance of radiant slab systems with free-hanging acoustical clouds

Caroline Karmann[1,*], Fred S. Bauman[1], Paul Raftery[1], Stefano Schiavon[1], William H. Frantz[2], Kenneth P. Roy[2]

[1] Center for the Built Environment, University of California, Berkeley, CA, USA
[2] Armstrong World Industries, Lancaster, PA, USA

[*]*Corresponding email: ckarmann@berkeley.edu*
Keywords: Cooling capacity, Radiant systems, Acoustical coverage, Reverberation time, Architectural acoustics

Abstract
Radiant slab systems have the potential to achieve significant energy savings, yet, when applied in the ceiling (e.g., thermally activated building system) the exposed concrete may also create acoustical challenges due to the high reflectivity of the hard surface. Balancing all of the building indoor environmental quality factors is important in the design of an effective workspace for the occupants, and so we need to consider the interactions between thermal and acoustic comfort. We assessed the cooling capacity in a hydronic test chamber and the sound absorption in a reverberation chamber to study the effects, for an office room, of different coverage areas of free-hanging acoustical clouds below a radiant chilled ceiling. The cooling experiments showed that for 47% cloud coverage of the ceiling area, we measured only an 11% reduction in cooling capacity caused by the blockage of radiant exchange between the ceiling and the room. The acoustical results showed that if the cloud covered 30% of the ceiling in a private office or 50% in an open plan office, acceptable sound absorption at the ceiling was achieved. We showed that good acoustic quality can be achieved with only a minor reduction of cooling capacity.

1 Introduction
Radiant slab systems have the potential to achieve significant energy savings primarily due to the use of lower temperature differences between the space and the heating or cooling source and the possibility to store energy in the slab [1]. This allows for higher efficiency at the device that generates hot or cold water, such as a boiler or chiller. In some cases, the relatively lower chilled water temperatures may eliminate the need for a chiller altogether, thereby enabling the use of non-refrigerant cooling sources, such as ground water, cooling towers, or indirect evaporative coolers. The use of water as the circulating fluid instead of air also reduces the energy costs of transferring heat to or from the space. Lastly, the thermal inertia inherent in a radiant slab system also provides opportunity for peak demand reduction and load shifting [2]–[6], [1]. However, the low temperature differences require large surfaces to ensure heat exchange with the space. As a result, designers typically implement radiant systems on the largest surfaces in the space (e.g., ceilings or floors).

By definition, a radiant heating and cooling system exchanges at least 50% of its heat through thermal radiation [7]. Radiant heat exchange between surfaces involves view factors, which represent the proportion of the radiation that leaves a first surface that strikes a second surface. To preserve heat transfer (and avoid compromising view factors), it is desirable to keep radiant systems uncovered. In the case of a commercial building, this is in direct conflict with the need to add acoustic absorption in the ceiling plane to improve the acoustic quality of the space. A suspended acoustical ceiling is the least expensive approach to adding sound absorption but it also requires a large surface area to be effective for reverberation control within the space. Practitioners have identified this conflict as a barrier for the implementation of radiant systems [8]. Occupant satisfaction studies conducted in buildings using radiant systems are commonly showing lower acoustic satisfaction compared to non-radiant buildings [9] proving that acoustic quality in buildings using radiant systems needs to be addressed.

All materials have the ability to absorb and reflect sound. Acousticians refer to the sound absorption coefficient as an indicator of the fraction of sound energy absorbed by a surface. Sound absorption coefficients depend on frequency and their value varies between zero (a perfectly reflective surface) and one (a perfectly absorptive surface). Massive radiant types such as thermally active building systems (TABS) are made of exposed concrete, whose sound absorption coefficients are typically 0.02 over the normal frequencies [10]. This means that TABS cause excessive sound reflection in spaces, which yield too much reverberation. By contrast, porous sound absorbing materials have sound absorption coefficients typically ranging between 0.30 and 0.90 depending on frequencies and types [10]. Sound absorbing material reduce both the sound level and reverberation time, which are key factors in the design of offices for acoustic comfort.

In this study, we wanted to address the problem of poor sound absorption of TABS. We proposed to combine a radiant cooled ceiling with several configurations of free-hanging discontinuous acoustic clouds (sometimes called canopies). This type of sound absorber is known to have an increased acoustic performance compared to regular suspended ceilings due to the larger surface area exposed to sound, i.e., both the upper and lower surfaces, since sound has access to both sides of the cloud. For simplicity, when referring to ceiling coverage for these clouds, we report the perpendicular projection of the cloud on the total ceiling area. It has been reported that covering 60% of a ceiling with free-hanging cloud can have comparable performance to 100% coverage with a suspended ceiling [11]. As they are free-hanging, these clouds have an open air space above them. Air can freely circulate between the cloud and the ceiling allowing heat exchange by convection from the radiant cooled ceiling.

The combination of radiant cooled ceiling with free-hanging acoustic clouds has raised research interest over the last decade, but we did not find experimental-based peer-reviewed journal publications on this topic. The conference papers and manufacturer white papers that we found consistently showed that the reduction of cooling capacity between slab and room was small and lower than expected [12], [13], [11], [14], [15]. Overall, it appears that partial coverage of a radiant chilled ceiling with free-hanging clouds does not cause a proportionally equivalent reduction of the cooling capacity. Instead, the reduction in cooling capacity is 3-4 times lower than the percentage cloud coverage. This outcome opens doors to the potential combination of acoustical clouds with TABS.

The objectives of this study are to: (1) experimentally assess the effect on radiant ceiling system cooling capacity for various coverage areas of free-hanging acoustic clouds, and (2) determine the change in sound absorption for the same configurations. We conducted two laboratory studies: the first one in a certified controlled climatic chamber equipped with a radiant cooled ceiling and free-hanging clouds, and the second one in a certified reverberant chamber equipped with comparable configurations of acoustic clouds.

2 Method

2.1 Cooling capacity measurements

2.1.1 Experimental facilities and room description

We conducted the cooling capacity experiments in a climatic chamber (4.27 m × 4.27 m × 3.0 m) at Price Industries in Winnipeg, Manitoba in September 2015. The floor area of the chamber is 18.2 m^2, and the volume is 54.7 m^3. The chamber has no windows. The walls, the ceiling, and the floor have similar construction and thermal properties with an overall conductance of 0.135 W/m^2K. Starting from the exterior the detailed wall composition includes: 3.522 m^2K/W insulation, a stagnant 0.102 m air gap (0.352 m^2K/W), aluminum extruded walls, 0.102 m of polyurethane board (3.522 m^2K/W). This chamber is accredited by the EN 14240 [16] for chilled ceiling testing. It is located inside a large laboratory facility maintained at 21.6º C ± 0.5º C (we note that the facility temperature was not measured for the test with highest coverage (71%), which was the first experiment conducted).

We installed graphite metal radiant panels in the chamber as part of a suspended ceiling placed at a height of 2.5 m above the floor. Each radiant panel is 1.83 m long and 0.61 m wide (area equal to 1.11 m^2). Cotton fiber insulation was placed on top of the panels (2.288 m^2K/W). In total, twelve radiant ceiling panels were centered on the ceiling, covering 73.5% (13.4 m^2) of the total area. The twelve panels were the maximum number that could be accommodated in the chamber. The intention was to represent TABS, the system of interest in this study, as near as possible by covering close to 100% of the ceiling area. We connected the panels in series in order to reduce overall measurement uncertainty (we reached lower uncertainty by increasing the temperature difference between supply and return water temperature). To ensure a more uniform distribution of surface temperatures at the ceiling level, the panels were connected in mixed order so that the average temperature of adjacent panels was similar. The chamber did not include an air system because we wanted to specifically focus on the change in cooling capacity of the radiant chilled ceiling, and adding an air system would increase overall uncertainty in the results.

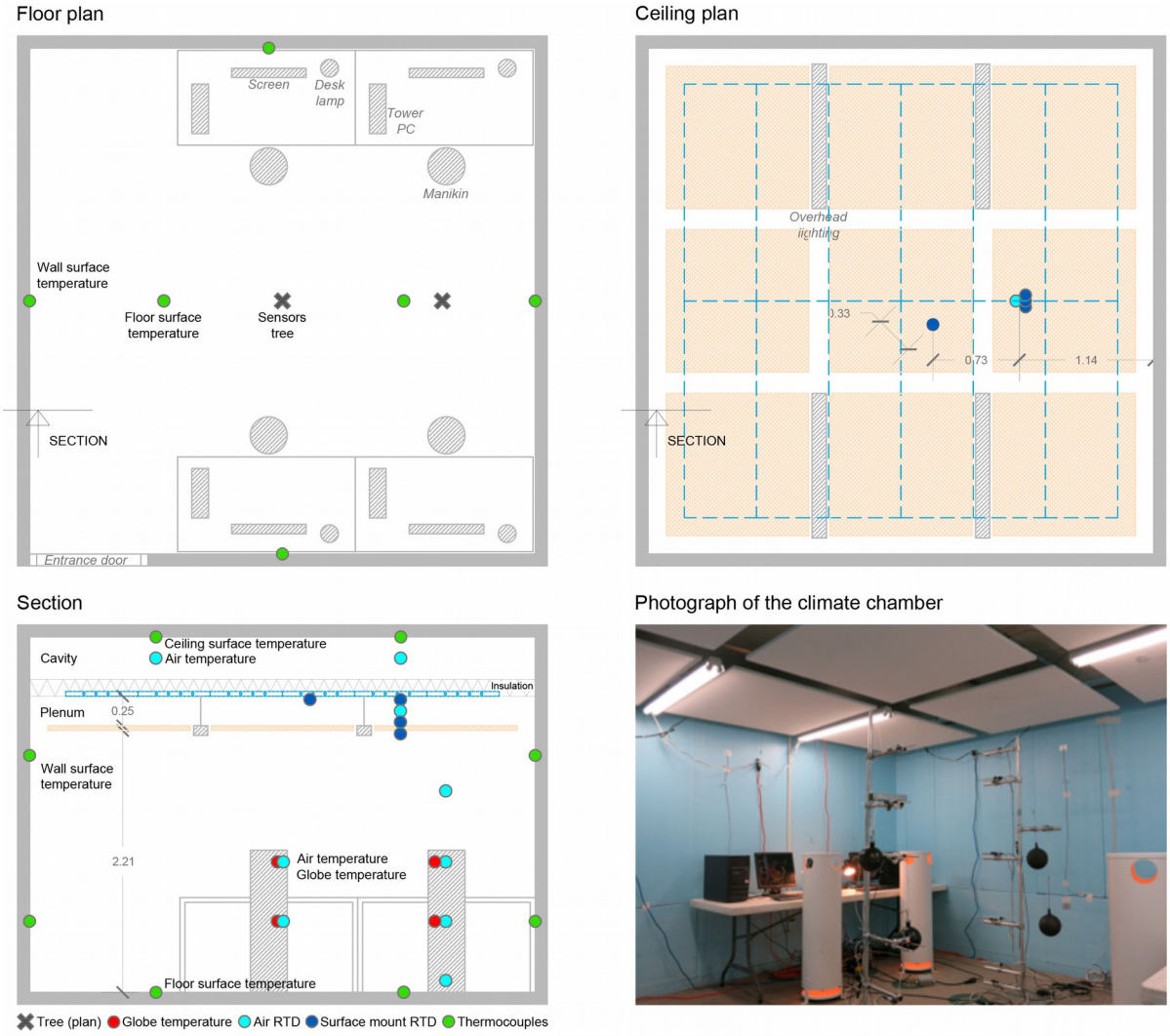

Figure 1: Plan, section and photograph of test chamber with sensors and cloud coverage. The acoustical clouds are in orange, the radiant ceiling in blue and the furniture/equipment in gray.

Table 1 summarizes the heat sources used in the experiment. We modeled office heat sources using computers (tower CPUs), flat screens and desk lamps on the desks, and overhead lighting (0.25 m below the radiant ceiling). We simulated occupants with power-adjustable dummies according to EN 14240 [16]. When fully installed, the test chamber represented a four-person office with a computer at each workstation; a relatively high occupant density of 4.55 m^2 per person. The data acquisition system was located outside the chamber, and therefore not listed here.

Table 1: Heat load summary

Heat source	Number	Total power (W)	Power per floor area (W/m^2)	Percent of total (%)
People (dummies)	4	300	16.5	27%
Computers	4	300	16.5	27%
Desk lamp and screens	4	283	15.5	26%
Overhead lighting	4	214	11.8	20%
Total		1097	60.3	100%

We also equipped the chamber with acoustical panels made out of fiberglass pre-formed in a 1.20 m square and 0.04 m thick cloud shape. These clouds were suspended at 0.25 m below the radiant ceiling (similar to the overhead lighting) centered on the ceiling in a 3 by 3 array, 1.37 m center to center. A maximum of 9 clouds could be positioned on the ceiling with a spacing of 0.17 m between them and 0.16 m between them and the walls. The overhead lighting fixtures could fit in the space in between two clouds. Figure 1 shows a plan and a section of the chamber with locations of the four simulated workstations and instruments. Blue lines represent the area of the radiant ceiling and orange squares represent the acoustic clouds. Figure 1 also includes a photograph of the lab set-up with 9 clouds (71% coverage) in the room.

2.1.2 Experimental conditions and procedures

We used the operative temperature measured in the center of the room at 1.1 m as our reference temperature to determine the cooling capacity between the ceiling and the room. The operative temperature accounts for both convective and radiant heat exchange mechanism and it is also a reference for thermal comfort analysis. It is often suggested as the most appropriate reference temperature for total heat transfer coefficient calculations [17]. As this experiment did not include air movement, we approximated the operative temperature with the mean of the air and mean radiant temperatures. The mean radiant temperature was derived from the globe temperature with the following equation:

$$T_{mr}=\left[\left(T_{globe}+273\right)^4+2.5\cdot10^8\cdot v_a^{\,0.6}\cdot\left(T_{globe}-T_a\right)\right]^{1/4}-273 \qquad (1)$$

The heat exchange between the radiant ceiling and the room is expressed in Equation 1, where U_{cc} represents the cooling capacity coefficient in (W·m^{-2}·K^{-1}).

$$q_{cc}=U_{cc}A_{panels}\left(t_{op}-t_{w,m}\right) \qquad (2)$$

$$\text{with} \quad t_{op}=\frac{t_a+t_{mr}}{2} \quad \text{, and} \quad t_{w,m}=\frac{t_{w,s}+t_{w,r}}{2}$$

On the water side, the radiant system cooling rate is expressed as:

$$q_w=\acute{m}_w c_{pw}(t)\left(t_{w,r}-t_{w,s}\right) \qquad (3)$$

Under steady state conditions, the water in the radiant panels absorbs the electrical power of the heat sources, and thus:

$$P=q_{cc}=q_w \qquad (4)$$

By substituting (2) & (3) in (4), and rearranging:

$$U_{cc}=\frac{\acute{m}_w c_{pw}\left(t_{w,r}-t_{w,s}\right)}{A_{panels}\left(t_{op}-t_{w,m}\right)} \qquad (5)$$

We conducted all tests with the same water mass flow rate (220 kg/h ± 0.02%) and water supply temperature (15° C ± 0.01° C). As the internal loads were kept constant (1097 W) for the different variants, the water return temperature also remained constant for all the tests (19.2 ± 0.1° C). From equation (5), the remaining variable able to influence the cooling capacity is the operative temperature, which is the equilibrium temperature at which the room settles for a given variant of ceiling coverage under steady state conditions.

We recorded the data once each test had reached steady state conditions. We defined it as a difference of less than 0.05 °C between the mean of the most recent 60 30-sec samples against the mean of the 60 samples immediately prior for every temperature sensor used in this experiment. After recording the data we calculated: (1) the average temperatures in the occupied zone, and (2) the cooling capacity coefficient U_{cc} according to Equation 5.

The experimental sequence was partially randomized. We started with the tests that included the largest amount of clouds (9, 8 and 6 clouds), then conducted the test without coverage and ended with the tests with lowest coverage (4 and then 2 clouds). We also included in the experiments two duplications (6 and 0 clouds) that we ran after all other variants were completed.

2.1.3 Comparison with EN 14240

European Standard EN 14240 [16] provides a different methodology to determine the cooling capacity of radiant panels. The expression of the results is of the form: $k \cdot \Delta\theta^n$, where k is the characteristic constant, n the exponent and $\Delta\theta$ the temperature difference between mean cooling water temperature and the reference room temperature (which is the globe temperature, measured in the middle of the room at a height of 1.1 m above the floor). This formula is based on empirical observation and the n exponent is used to account for the non-linearity of radiant heat exchange.

We also used this method to determine the coefficients k and n for our tests. We also calculated a linear model for this equation (using the same $\Delta\theta$). We found that the two models were comparable at predicting the cooling capacity (R^2 of 0.98 for the power model and 0.97 for the linear model). This is due to the moderate range of temperatures in which radiant systems typically operate. As a result, we used a linear model in our analysis. Additionally, we note that the EN 14240 uses the globe temperature as the room reference. Globe temperature is an often used approximation to operative temperature, a relationship that breaks down under some conditions such as elevated air speed. Thus, we used the operative temperature as the room reference.

2.1.4 Instrumentation

Table 2 lists the instruments and equipment used in this experiment. The water supply and return temperatures of the radiant system, and the air temperatures on the trees in the chamber were monitored continuously with resistance temperature detector (RTD). We calibrated these prior to the experiment using a Fluke 1524 Reference Thermometer in a Fluke 9171 Metrology dry well calibrator (± 0.029 °C). We shielded air temperature sensors from radiant heat transfer using a reflective aluminium cylinder. At 0.6 m and 1.1 m height on both trees, the globe temperature was measured with a black-globe thermometer. The black-globe thermometer fulfills the requirements of ISO 7726 [18]. We used RTDs to measure the temperatures of the surface of the radiant panels (above and below) and of the acoustical clouds for a few locations. We measured the inner surface temperatures of the ceiling, floor and vertical walls (12 in total, and two for each wall) using thermocouples. The accuracy obtained after calibration for each type of sensor is reported in Table 2. The electrical power was measured with a Fluke 41 power harmonic analyzer. Figure 1 shows the location of the sensors in plan and section view.

Table 2: List of sensors and specifications for the cooling capacity measurements

Instruments	**Accuracy**	**Unit**	**Measured variables and sensor location**
Air RTD	±0.07	°C	Air temperatures:
Omega Air RTD PR-25AP-1/10			- 2 trees at 0.1, 0.6, 1.1, 1.7 m
DIN			- below the radiant panels and above the clouds

			Globe temperatures: - 2 trees at 0.6 and 1.1 m
Water RTD Omega 1/10 DIN	±0.07	°C	Supply and return water temperatures
Surface Mount RTD Omega Class A Platinum RTD	±0.15	°C	Upper and lower sides of the radiant panels Upper and lower sides of the acoustical clouds
Thermocouples Omega Type J 24 Gauge Thermocouple Wire	±0.15	°C	Wall surface temperatures Floor and ceiling surface temperature
Anemometer TSI 8475 Velocity Sensors	±3.0 of reading +1% of full scale	%	Central tree at 0.6 and 1.1 m Side tree at 0.1, 0.6, 1.1 and 1.7 m
Water Flow Meter Siemens Sitrans Massflo2100 Coriolis Meter	±0.02	%	Radiant cooling panel water flow rate

2.1.5 Uncertainty

We analysed the data in accordance with the ISO 13005 [19] and the JCGM 100 guidelines [20] for the expression of uncertainty. The uncertainty in a primary measurement is estimated as the root sum of the square of the uncertainties. The uncertainty due to an individual source of error can be instrument uncertainty, random error due to spatial variation (when averaging spatially distributed sensors), and error from data acquisition system, etc. For each type of measure, the global expanded uncertainty was evaluated according to ISO 13005 with a level of confidence of 95% (coverage factor at k = 2). Error bars represent the uncertainty when presented on the graphs.

The uncertainty of the mean radiant temperature is of the form:

$$u_{t_{mr}} = \sqrt{\left(\frac{\delta t_{mr}}{\delta t_{globe}}\right)^2 u_{t_{globe}}{}^2 + \left(\frac{\delta t_{mr}}{\delta v_a}\right)^2 u_{v_a}{}^2 + \left(\frac{\delta t_{mr}}{\delta t_a}\right)^2 u_{t_a}{}^2} \qquad (6)$$

with:

$$\frac{\delta t_{mr}}{\delta t_{globe}} = \frac{2.5\cdot 10^8 \cdot v_a{}^{0.6} + \left(t_{globe}+273\right)}{4\cdot\left[\left(t_{globe}+273\right)^4 + 2.5\cdot 10^8 \cdot v_a{}^{0.6}\cdot\left(t_a - t_{globe}\right)\right]^{3/4}}$$

$$\frac{\delta t_{mr}}{\delta v_a} = \frac{37.5\cdot 10^6 \cdot \left(t_{globe} - t_a\right)}{v_a{}^{0.4}\cdot\left[\left(t_{globe}+273\right)^4 - 2.5\cdot 10^8 \cdot v_a{}^{0.6}\cdot\left(t_a - t_{globe}\right)\right]^{3/4}}$$

$$\frac{\delta t_{mr}}{\delta t_a} = \frac{62.5\cdot 10^6 \cdot v_a{}^{0.6}}{\left[\left(t_{globe}+273\right)^4 + 2.5\cdot 10^8 \cdot v_a{}^{0.6}\cdot\left(t_{globe} - t_a\right)\right]^{3/4}}$$

The uncertainty of the radiant system cooling rate can be approximated by:

$$u_{q_w} = c_{pw}(t)\sqrt{\left(\acute{m}_w u_{\Delta t_w}\right)^2 + \left(\Delta T_w u_{\acute{m}_w}\right)^2} \qquad (7)$$

with: $\Delta T_w = t_{w,r} - t_{w,s}$, and $u_{\Delta T_w} = \sqrt{\left(u_{t_{w,s}}\right)^2 + \left(u_{t_{w,r}}\right)^2}$

The uncertainty in the cooling capacity coefficient U_{cc} is of the form:

$$u_{U_{cc}} = \sqrt{\left(\frac{\delta U_{CC}}{\delta \acute{m}_w}\right)^2 u_{\acute{m}_w}{}^2 + \left(\frac{\delta U_{CC}}{\delta t_{w,s}}\right)^2 u_{t_{w,s}}{}^2 + \left(\frac{\delta U_{CC}}{\delta t_{w,r}}\right)^2 u_{t_{w,r}}{}^2 + \left(\frac{\delta U_{CC}}{\delta T_{op}}\right)^2 u_{t_{op}}{}^2} \qquad (8)$$

with:

$$\frac{\delta U_{CC}}{\delta \acute{m}_w} = \frac{c_{pw}\left(t_{w,r} - t_{w,s}\right)}{A_{panels}\left(t_{op} - \frac{t_{w,r} + t_{w,s}}{2}\right)}$$

$$\frac{\delta U_{CC}}{\delta t_{w,s}} = \frac{\dot{m}_w c_{pw}\left(t_{op} - t_{w,s}\right)}{A_{panels}\left(t_{op} - \frac{t_{w,r}+t_{w,s}}{2}\right)}$$

$$\frac{\delta U_{CC}}{\delta t_{w,r}} = \frac{\dot{m}_w c_{pw}\left(t_{w,r} - t_{op}\right)}{A_{panels}\left(t_{op} - \frac{t_{w,r}+t_{w,s}}{2}\right)}$$

$$\frac{\delta U_{CC}}{\delta t_{op}} = \frac{-\dot{m}_w c_{pw}\left(t_{w,r} - t_{w,s}\right)}{A_{panels}\left(t_{op} - \frac{t_{w,r}+t_{w,s}}{2}\right)}$$

The sample uncertainties of the derived quantities (water temperature differences, cooling load removed by the panels, and the cooling capacity coefficient U_{cc}) have been evaluated based on the equations above. The derived uncertainties for the total cooling load and for U_{cc} were respectively 4.9% and 5.1% (maximum values).

2.1.6 Variant description

We tested 6 different levels of acoustical coverage: 0% (0 clouds), 16% (2 clouds), 32% (4 clouds), 47% (6 clouds), 63% (8 clouds) and 71% (9 clouds). Figure 2 (left) shows the location of the clouds for each level. The reference case for the study is the variant without acoustical coverage. For cooling capacity testing of the variant with highest acoustical coverage (71%), by mistake additional heat load of 43 W (4% of the total internal load) occurred at the wall level due to the operation of guard heaters in the wall. These heaters were not used in any other tests. This additional load did not affect the cooling capacity results but it did modify wall mean surface temperature. Thus, not all results are represented for this variant.

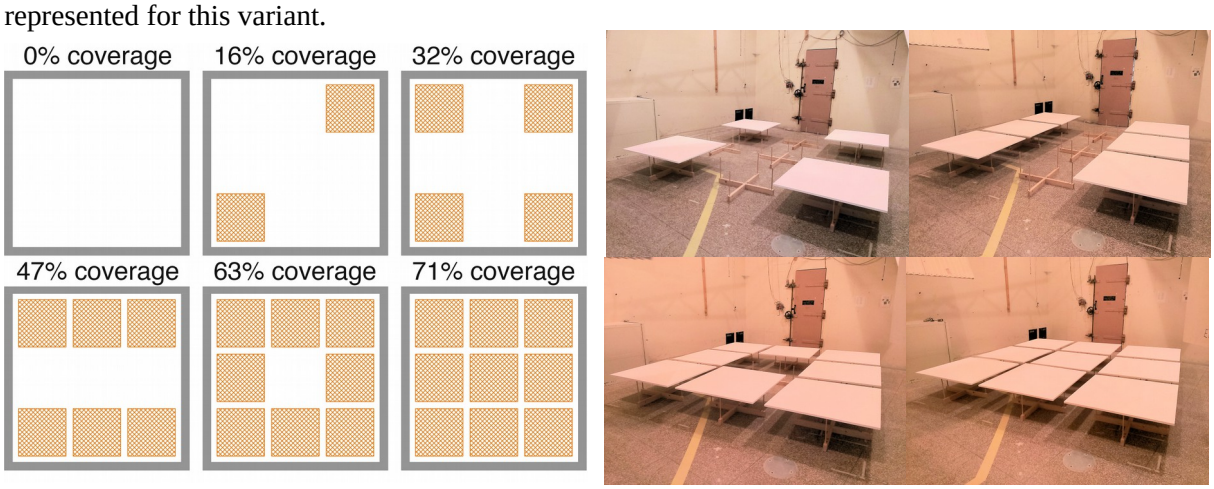

Figure 2: (Left) Schematics of coverage going from 0% to71% (as tested in the climatic chamber) (Right) Series of 4 photographs taken in the reverberation chamber with 4, 6, 8 and 9 clouds.

2.2 Sound absorption measurements

2.2.1 Experimental facilities and test room description

We conducted the sound absorption experiments in a reverberation chamber (6.22 m × 8.17 m × 5.22 m) at Armstrong World Industries in Lancaster, PA in August 2015. This chamber is accredited by the NVLAP (National Voluntary Laboratory Accreditation Program (USA)) for sound absorption testing following ASTM Standard C423 - 09a [21]. The walls are constructed of 0.2 m concrete block with filled cavities, and the ceiling is reinforced concrete. Both the wall and ceiling surfaces are

painted with an epoxy paint. The floor is reinforced concrete topped with terrazzo tile. The test room sits on springs on independent foundations from the surrounding building.

2.2.2 Experimental conditions and procedure

The sound absorption of a test sample is based on the measurement of a decay rate within the reverberation chamber. We conducted these measurements according to ASTM Standard C423 [21]. For this testing, a broadband random noise signal is turned on long enough for the sound pressure level to reach steady state. When the signal is turned off, the sound pressure level decreases and the decay rate in each frequency band is determined by measuring the slope of a straight line fitted to the sound pressure level of the average decay curve. Typically 50 to 60 measured decays are averaged to meet the precision requirements of the test code. This decay curve is adjusted by subtracting the sound absorption of the empty room itself including that due to air. The sound absorption is calculated based on the Sabin formula:

$$A_{absorption} = 0.9210 \frac{V\,d}{c} \qquad (9)$$

where A is the equivalent sound absorption area in [Sabin, m^2], V the volume of the reverberation room in [m^3], c the speed of sound in [m/s], and d the decay rate in [dB/s].

2.2.3 Instrumentation

To comply with the methodology prescribed in the ASTM C423, we used the following measuring instruments: microphones, pre-amplifiers for those microphones, temperature/humidity sensor, barometric pressure sensor, speakers, and data collection hardware. Table 3 summarizes the sensors and electronic equipment.

Table 3: List of sensors and specifications for the acoustical measurements

Instruments	**Unit**	**Measured variables and sensor location**
Microphones Bruel & Kjaer Model 4176	6	microphones randomly located in the reverberant room
Preamplifiers Bruel & Kjaer Model 2669,	6	preamplifiers connected to the microphones
Temperature/RH sensor Vaisala HMP 231	1	Sensor located on the North wall of reverberant room
Barometric Pressure Sensor Setra Model 370	1	Sensor physically located in the control room (input connected by 6.35 mm tubing to the chamber)
Speakers Soundsphere Q-15 speakers	1	Speakers located in the upper NW and SE corners of the room
Data Collection hardware Bruel & Kjaer Multi-Analyzer modules - Model 3050-A-040	2	Data Collection hardware located in the control room
Data Collection hardware Bruel & Kjaer Multi-Analyzer modules - Model 3160-A-022	1	Data Collection hardware located in the control room

2.2.4 Uncertainty

The reverberation chamber is certified by the ASTM C423. The uncertainty is based on the methodology given in Section 13 of ASTM C423 listing the 95% probability limits for repeatability of the sound absorption measurements in this test chamber.

2.2.5 Variant description

We used the same acoustic cloud for the cooling capacity and acoustic testing. These acoustical panels are fabricated of a fiberglass pre-formed into a 1.20 m square by 0.04 m thick cloud shape (Armstrong Soundscapes Shapes). Figure 2 (right) shows the four acoustical cloud configurations tested in the reverberation chamber (using 4, 6, 8 and 9 clouds). As with the cooling capacity testing, up to 9 clouds were positioned into a 3 by 3 array, 1.37 m center to center. The tests were conducted with the panels raised above the floor (as opposed to suspended), and the distance to the floor is equivalent to plenum depth if suspended. In these acoustic tests the height was 0.40 m (note that a suspension distance of 0.25 m was used in the cooling capacity testing).

2.2.6 Complementary analysis

The output of the acoustic testing per ASTM C 423 is the sound absorption as reported in metric Sabin (Sabin, m^2). In order to understand the effect of the clouds in a more realistic setting, we used this output to model the reverberation time (T_{60}) of a typical closed office space. The reverberation time is defined as the time it takes for a sound, such as a loud hand clap, to dissipate after being made by a level reduction of 60 dB. It is commonly abbreviated T_{60} in seconds (s), and it can be calculated for each frequency using the Sabine formula:

$$T_{60} = 0.161 \frac{V}{A_{absorption}} \qquad (10)$$

with A, equivalent sound absorption area in [Sabin, m^2], and V, volume of the room in [m^3].

We modelled an office with comparable characteristics as for the cooling capacity testing. We assumed an 18.2 m^2 room with a floor to ceiling height of 2.65 meters (the cooling capacity test room has 2.50 m floor to ceiling height, and so, the plenum depth in the acoustic testing was 0.15 m deeper). We further assumed a concrete finish ceiling (for the base case with no clouds), plaster on the walls, and a light carpet on the floor. We assumed a furnished but unoccupied space. We assumed wooden panels for the entrance door and the desks and three lightly upholstered chairs. The sound absorption coefficient of these materials and finishes are reported in .

Table 4: Sound absorption coefficient used for reverberation time calculation

Surface	**Materials**	**Qu.**	**Unit**	**Octave Band (Hz)**					
				125	**250**	**500**	**1000**	**2000**	**4000**
Ceiling	Concrete[(1) (4)]	18.1	m^2	0.01	0.01	0.02	0.02	0.02	0.02
Walls (door subtracted)	Plaster (gypsum on wood lath) [(1)]	43.4	m^2	0.12	0.09	0.07	0.05	0.05	0.04
Floor	Carpet (up to 0.006m pile height)[(2)]	18.1	m^2	0.02	0.04	0.06	0.20	0.30	0.35
Door and desks	Wood [(2)]	6.4	m^2	0.10	0.08	0.06	0.05	0.05	0.05
Chair	Lightly upholstered chairs[(3)]	3	items	0.35	0.45	0.55	0.60	0.60	0.60

[(1)] Source: [10], [(2)] Source: [22], [(3)] Source: [23], [(4)] We used concrete ceiling as the reference case because this is the typical finish for TABS

Reverberation time criteria are published by ASHRAE in the Performance Measurement Protocols (PMP) Best practices Guide [24] and can be used to determine what acoustical cloud coverage may be needed. Reverberation time relates to speech clarity, and low reverberation (on the order of 0.6 or 0.8 seconds depending on office type) is usually desirable for speech intelligibility.

3 Results

We present the results separately below for the cooling capacity and the sound absorption testing. For the cooling capacity testing, we include further results on thermal comfort. The sound absorption results also include T_{60} derived from the measurements and calculated for a typical (furnished but unoccupied) closed office.

3.1 Cooling capacity testing

Table 5 summarizes the main results of the testing. The chamber reached steady-state equilibrium at an operative temperature between 26.5º C (no coverage) and 29.3º C (71% coverage).

Table 5: Experimental results for parameters

Coverage	t_a [1] (º C)	t_{mr} [1] (º C)	t_{op} [1] (º C)	$t_{w,r} - t_{w,s}$ (º C)	$t_{w,m}$ (º C)	q (W)	q'' [2] (W/m²)	q'' [3] (W/m²)	U_{cc} [3] (W/(m².K))	*Change in* U_{cc} [3] (%)
0%[4]	27.1	26.0	26.5	4.2	17.1	1069	79.8	58.7	8.46	100%
16%	27.2	26.4	26.8	4.2	17.1	1067	79.7	58.6	8.19	97%
32%	27.2	26.7	27.0	4.1	17.1	1054	78.7	57.9	7.93	94%
47%[4]	27.9	27.3	27.6	4.1	17.1	1061	79.2	58.3	7.54	89%
63%	28.0	28.1	28.0	4.1	17.0	1041	77.7	57.2	7.06	83%
71%	29.1	29.5	29.3	4.3	17.2	1112	83.0	61.1	6.85	81%

[1] Measured at the central tree at 1.1 m. high; [2] Per unit of panel area; [3] Per unit of floor area; [4] Replicated experiment

3.1.1 Cooling capacity coefficient

Figure 3 shows the change in cooling capacity coefficient (U_{cc}) at each level of cloud coverage. We observe that adding coverage reduces this coefficient. Yet, this reduction is small compared to the coverage: the cooling capacity coefficient only decreases by 3.2% for 16% coverage and by 19% for 71% coverage. The reduction in cooling capacity coefficient is on average 4 to 5 times lower than the percentage coverage. This result generally confirms the trend observed in the literature but with a slightly larger difference between cooling capacity coefficient and coverage, depending on the reference. The difference in cooling capacity between the replicated tests, performed non-sequentially, was 0.25% and 0.04% for the 0% and 47% coverage cases, respectively. This indicated that the lab is very reliable and provides reproducible results.

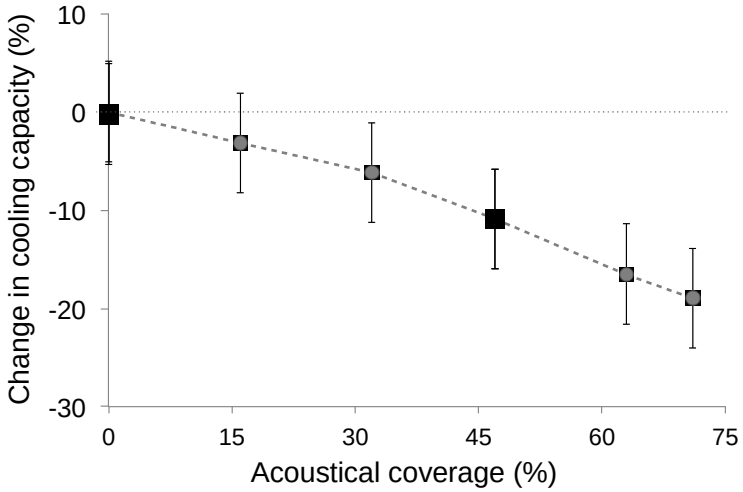

Figure 3: Change in cooling capacity coefficient (U_{cc}) as a function of acoustical coverage. The grey dots show the main results of the testing. The black "ex" represents replications

3.1.2 Thermal comfort

Figure 4A shows the difference between air and mean radiant temperatures measured at 1.1 m high as a function of acoustical coverage. Both the central and the side measurement trees are represented. For both locations and with lower coverage, the air temperature is slightly higher than the mean radiant temperature. We note that in the case of air systems, this difference is commonly greater [25]. As the coverage increases, the difference between both temperatures diminishes and the mean radiant temperature eventually gets slightly higher than the air temperature. We can hypothesize that the share of heat transfer exchange between the panels and the sensors becomes more convective and less radiative. Between 16% and 71% coverage, the air and mean radiant temperatures stay within 1º C of each other. For the tree close to the wall, the difference between the two temperatures is always less than 1º C. This is an important observation. Differently from air systems, in radiant systems the air and mean radiant temperature are quite similar, therefore, if these results are confirmed in field tests, we may infer that an operative temperature sensor is not needed for control purposes, an an air temperature sensor will be sufficient. With no obstruction, the difference between air and mean radiant temperatures is 0.6º C lower for the side tree compared to the central tree, even though the two trees are only 1.35 m apart from each other. At neutral comfort condition, a change of 0.6º C equals 0.2 PMV or 0.11 clo. This change is comparable to the effect of a shirt (slightly more than a T-shirt). This mean radiant temperature reflects the influence of the wall temperature (warmer than the ceiling) and it shows the importance of view factor. This point also brings the question of the location of sensors in rooms. Close to the wall, where the thermostat is usually located, the two temperatures are even closer, supporting the hypothesis that an operative sensor may not be needed. With higher coverage, we note that air and mean radiant temperature are overall getting closer to each other. Using the operative temperature (or even the air temperature) to control a radiant system with coverage is going to be more accurate compared to a radiant system without coverage. Figure 4B shows the difference in average surfaces temperature between walls and radiant ceiling as a function of acoustical coverage. As the coverage increases, this difference increases: the active ceiling temperature stays constant at around 21.6º C ± 0.3º C while the wall temperatures rise continuously from 26.8º C to 28.3º C. Thus, the difference in average surface temperatures between wall and ceiling is mainly due to the effect of the wall temperatures. As coverage increases, the view factor from the ceiling to the walls decreases, which impacts the wall temperatures and further the mean radiant temperature. Considering a larger office and in the case of no coverage, the cooler ceiling temperature will have a bigger influence on the mean radiant temperature in the center of the room. The difference between the air and the mean radiant temperature will increase compared to what we measured and reported in Figure 4A. In this regard adding coverage may bring a steeper slope than the one observed here in Figure 4A.

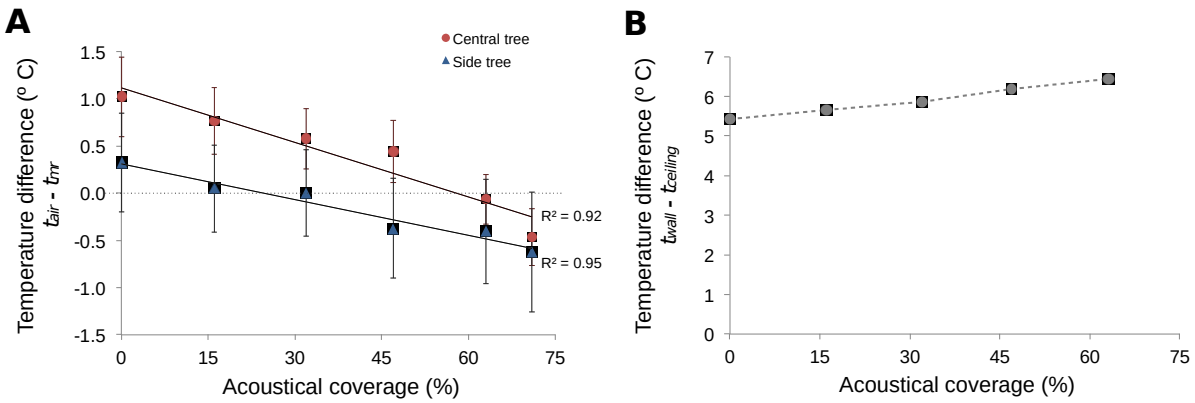

Figure 4: (A) Difference between air and mean radiant temperature (central and side trees at 1.1 m height) as a function of acoustical coverage, (B) difference in average surface temperature between wall and ceiling as a function of acoustical coverage

3.2 Acoustic absorption

3.2.1 Sound absorption

Table 6 summarizes the main results of the acoustic testing from the reverberation chamber measurements presented as sound absorption for each cloud configuration by normalized octave band frequency. This absorption is obtained by subtracting the absorption of the bare room from the treated room.

Table 6: Sound absorption of each cloud configuration in Sabin, m^2

Number of clouds	Octave Band (Hz)							
	63	**125**	**250**	**500**	**1000**	**2000**	**4000**	**8000**
4	0.3	2.1	5.1	5.7	8.2	10.0	10.1	9.2
6	0.3	2.3	7.2	8.1	11.5	13.8	13.7	12.8
8	0.7	3.8	9.5	10.2	14.5	17.5	17.3	16.0
9	1.0	4.8	9.9	10.8	15.8	18.3	18.5	16.7

3.2.2 Reverberation time

The reverberation time, T_{60} is defined as the length of time required for the sound level in a room to fall by 60 dB after the sound was made. The reverberation time is directly proportional to the room volume, and inversely proportional to the sound absorption properties of its walls, floor, ceiling, and its furnishings, as well as the air absorption. To complete our acoustical assessment, we calculated T_{60} for a closed office based on the sound absorption of our variants and on additional assumptions reported in section 2.2.6. The ceiling surface area is the same as for the cooling capacity section. Therefore, the number of clouds aligns with the percent cloud coverage reported previously and we will report the results based on coverage. The total absorption of the ceiling for the reference case (concrete ceiling) was calculated using the sound absorption coefficient (reported in) multiplied by the actual ceiling surface (18.1 m^2). The values for the 32%, 47%, 63% and 71% coverage were directly taken from Table 6 (4, 6, 8 and 9 cloud variants). For the 16% coverage, we did an extrapolation based on the experimental results obtained for the 4, 6 and 8 clouds variants and on coverage. Additionally, we looked for standards and guidelines to find recommended values for the T_{60} in offices. We found maximum recommended values for open-space office (0.6 s.) and private office (0.8 s.) in the ASHRAE PMP Best practices Guide [24]. These values are reported on the graphs for comparison.

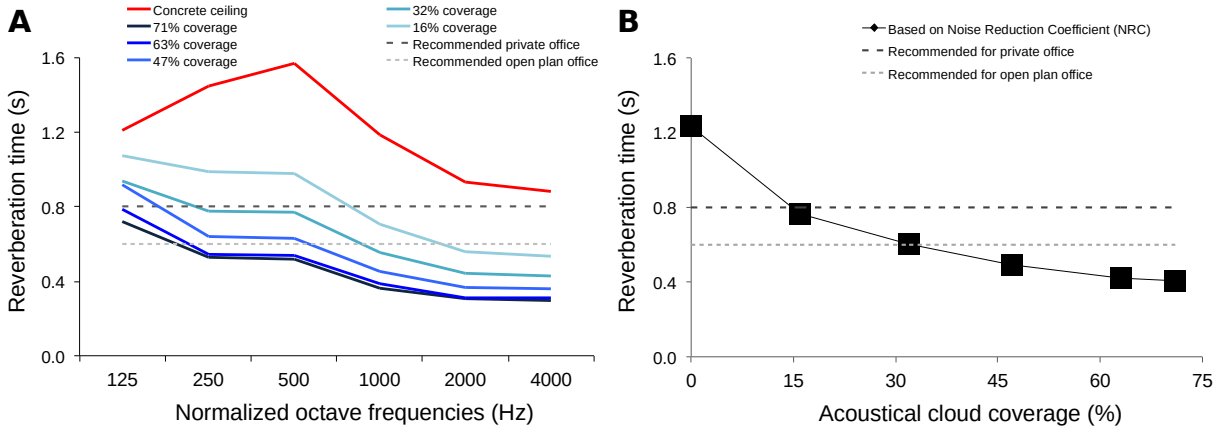

Figure 5: (A) Reverberation time as function of frequencies for different acoustical cloud coverage, and (B) reverberation time as a function of coverage based on the Noise Reduction Coefficient (NRC)

Figure 5 (A) shows the result of this analysis. T_{60} is shown as a function of frequency for different acoustic coverage. We observe that adding acoustical clouds in the ceiling plane strongly reduces the reverberation time. The peak of 1.6 s at 500 Hz for the concrete variant (base case) drops to 1 s for 16% coverage, 0.8 s for 32% coverage, 0.6 s for 47% coverage and down to 0.5 s for 71% coverage. With 32% coverage, the room meets the recommended values for private offices for most of the frequencies. Figure 5 (B) shows the T_{60} as function of acoustical cloud coverage. For this figure, we used the single-value Noise Reduction Coefficient (NRC) that is determined by calculating the mean value from the four octave values of the sound absorption coefficient between 250 Hz and 2000 Hz, and rounded the result to the nearest 0.05. One limitation of this average is that frequencies below 250 Hz (that include the human voice for instance) are not taken into account. Nevertheless, this single-value allows us to visualize the effect of acoustical coverage for an average sound absorption of the material. Based on these recommended values, we can conclude that: (1) even low cloud coverage (around 15%) can considerably improve acoustic absorption compared to a concrete ceiling; (2) covering 30% of the ceiling with an acoustical cloud would provide an acceptable absorption in the private offices, and (3) covering 50% of the ceiling with an acoustical cloud would provide an acceptable absorption in open plan offices. This study was focused on specific cloud configurations for the ceiling. The office simulation was built with sound reflective surfaces. Different plenum heights and different spacing between the clouds or such configuration in a different space may yield different results.

4 Discussion

The purpose of this study was to conduct laboratory experiments for a closed office space with different percent coverage of free-hanging acoustical clouds below a thermally activated building system to look at the interactions between thermal and acoustical factors. We used a hydronic test chamber to investigate the cooling capacity of the TABS, and a reverberation chamber to determine the sound absorption of our acoustical cloud variants. We wanted to simulate comparable variants for both experiments, and for the cooling capacity testing we could directly simulate an office room. For the acoustical testing, we tested the sound absorption of the different ceiling variants, and used this output to calculate the reverberation time of an office space. We assumed a similar space for the thermal and acoustical testing.

We conducted the cooling capacity experiment in a chamber equipped with radiant metal panels. Yet, with our experiment, we were trying to address the case of TABS. Unlike radiant panels, TABS typically cover a larger area leaving less space for acoustical treatment. In our experiments, most of the ceiling (73.5%) was covered with radiant panels, which is reasonably representative of the TABS system of interest in this study (we note that TABS do not typically cover the entire ceiling due to structural constraints). Additionally, the composition of radiant panel systems can offer the possibility to integrate acoustical treatment within the panel (e.g., using a perforated metal panel and adding insulation on the back). We did not consider these options and stayed with a plain non-perforated metal panel. We used a chamber equipped with radiant panels because we only had this option and this configuration allowed us to reach steady state condition faster. The emissivity of the two finished surfaces was comparable. Thus, the cooling capacity experiment applies to both radiant panels and TABS. Embedded surface systems (ESS) are another type of radiant system. ESS are comparable to TABS and therefore we can extend our cooling capacity results for this type of system under steady-state conditions. We performed our acoustical analysis with a simulated concrete ceiling because we wanted to address the case of TABS. As reported in Table 4, the acoustical absorption of concrete is extremely low. Using different materials or finishes on a radiant system yields comparable or better results.

With this experiment, we found that the cooling capacity coefficient only decreases by 3.2%, 11% and 19% for a ceiling cloud coverage of 16%, 47% and 71% respectively. We compared this outcome with the results found in the literature. With free-hanging acoustical clouds and a plenum of 0.2 m, Peperkamp and Vercammen [13] observed a reduction of the cooling capacity of ~20% for 50% coverage, Chigot [11] reported a reduction of ~16% for 45% coverage and Ecophon (acoustic material manufacturers) [15] reported a reduction of ~18% for 45% and of ~27% for 60% coverage. With a

larger plenum of 0.6 m, Weitzmann et al. [12] observed a reduction of the cooling capacity of ~30% for 83% coverage. Overall, though coverage and plenum height was not exactly the same as in previous experiments, we can state that the results of our experiment show less reduction in cooling capacity compared to what was previously reported.

It is important to underline that there is a difference between geometrical percentage of covered ceiling and occupant perception of ceiling coverage. It is unlikely that occupants will visually perceive the relatively narrow gaps between the acoustic clouds as open space. Therefore, the ceiling appears more covered than what it is. For example, from occupants and designers' perspective, 47% coverage is likely to be perceived as closer to two thirds of the ceiling and the 71% variant closer to the full ceiling being covered (see schematics Figure 2 (left)). What we describe in this paper as low coverage (16% and 32%) still represent a meaningful portion of the ceiling from a visual perception perspective.

We conducted this experiment for a cooling application. As the heat released by the internal loads rises, this configuration is also best to ensure higher natural convection and mixing near the ceiling. This creates an airflow cell in the room, counteracting the effect of stratification. It is unlikely that a heating application will show similar results as there would be stagnant, warmer air between the ceiling and the acoustic clouds. The share of convection compared to radiation would be lower than in the cooling application [26]. Thus, we would expect a stronger reduction in heating capacity with increasing coverage by the clouds. This heating application warrants further testing.

Cooling capacity experiments were conducted for a room with no ventilation system. We decided to focus on the change in cooling capacity due to acoustic coverage. Adding an air distribution system would bring multiple questions, including the type of system, location and type of diffusers, volumetric air flow and supply temperature. The design of the ventilation system may also impact the ratio of convective and radiative heat transfer close to the cooled ceiling surface. Air systems (particularly overhead mixing) will also likely increase surface convention [27] . The question of the interaction between the chilled ceiling and both coverage and ventilation system would be worth investigating.

The size of the laboratory chamber for the cooling capacity testing has an impact on the view factors between the ceiling and the sensors. Compared to a larger room (typical for open plan offices), our chamber has relatively small dimensions, leading to lower view factors to the ceiling (and floors) and higher view factors to the walls. In the case of a larger office, the ceiling temperature will have more effect on the mean radiant temperature than is the case for our chamber. Based on Figure 4B, the average ceiling temperature was about 6ºC lower than the average wall temperature. This difference is going to impact the mean radiant temperature taken in the center of the space for larger rooms. In the case of no coverage, the mean radiant temperature is going to be cooler than in the small office tested. Thus, we may expect the cooling capacity to be higher for the reference case (no coverage) in a large office. Due to the increased impact of the ceiling, it is likely that the percent reduction in cooling capacity would be slightly more important if tested in a larger office space. Overall we would expect this difference to be moderate. Also, this phenomenon can be counteracted by the presence of furniture, cubicles or other forms of partitions, depending on office layout and type.

Based on recommended values, we estimated that covering 30% of the ceiling with acoustical clouds would provide an acceptable absorption for private offices. In shared offices we would need to cover 50% of the ceiling. On the energy side, our experiment showed that 47% coverage would reduce the cooling capacity by about 11% in the case of the small office. This reduction may increase in the case of larger office but this change should not exceed a few percent. The application of radiant slab systems with free-hanging acoustical clouds in both small and large shared offices would mainly depend on the cooling requirements and on how much a 10-15% reduction of the cooling capacity may impact thermal comfort.

While the cooling capacity testing was mainly dependent on the coverage, the acoustic testing was also highly dependent on the type of product tested. Thus, it is important to note that the results

obtained for sound absorption and reverberation time are valid for these clouds (Armstrong SoundScapes) and similar types of absorbers. The plenum depth for the acoustic testing was 0.15 m greater than the plenum used in the cooling capacity testing. Also, the reverberant chamber was larger than the hydronic chamber and therefore, the walls were further away from the canopies being tested in the center of the space. Both the plenum depth and the distance to the walls may have slightly influenced the sound absorption values obtained at low frequency (a higher plenum and larger distance to the walls would help the sound to access and be absorbed on the back of the canopy). Yet, the acoustical analysis based on T_{60} calculation was rather conservative in its assumptions (lower sound absorption coefficient (see)), and therefore, the results are reasonable. We may also point out here that we tested horizontal clouds and not vertical baffles that may bring a different set of constraints between cooling capacity, sound absorption, ceiling appearance and perceived ceiling height.

The acoustic section of this article was focused on the absorption of the different panel configurations and on the reverberation time. Absorption at the ceiling is likely to provide only a partial answer to room acoustical problems. It addresses background noise level and reverberation time, but does not by itself solve sound privacy issues, which are perceived as one of the biggest constraints in open plan offices [28], [29]. Our experiment was able to show that combining a radiant chilled ceiling with free-hanging acoustical clouds can reduce reverberation issues while having a relatively modest impact on heat transfer. However, it is clear that additional modifications would be required for increased acoustical quality in shared office spaces.

5 Conclusions

We conducted laboratory experiments to investigate the change in cooling capacity and the sound absorption of an office room with different coverage areas of free-hanging acoustical clouds below a radiant cooled ceiling. The main conclusions of this study are:

- The cooling capacity coefficient only decreases by 3.2%, 11% and 19% for a ceiling cloud coverage of 16%, 47% and 71% respectively. This reduction is on average 4 to 5 times less than the percentage coverage.
- The difference observed between air temperature and mean radiant temperature is less than 1º C. This implies that measuring operative temperature or mean radiant temperature may not be needed in radiantly conditioned buildings. With lower coverage, the air temperature is slightly higher than the mean radiant temperature. As the coverage increases, the difference between both temperatures diminishes and the mean radiant temperature eventually gets slightly higher than the air temperature.
- The acoustical clouds exhibited the greatest sound absorption between 200 and 2500 Hz. The sound absorption per cloud slightly decreases with increasing number of clouds.
- Compared to exposed concrete, our tested cloud variants resulted in a substantial reduction of reverberation time. Even low cloud coverage (15-35%) can considerably improve sound absorption at the ceiling. The acoustic results showed that if the clouds covered 30% of the ceiling in a private office or 50% in an open plan space, acceptable sound absorption at the ceiling was achieved.

Overall, this study addresses one limitation often associated with radiant systems using exposed concrete ceilings, which is the question of can you achieve acceptable acoustical quality without overly compromising the cooling performance of the radiant ceiling. The results demonstrated a practical solution in which free-hanging acoustical clouds are positioned below a radiant chilled ceiling. The observed reduction in cooling capacity at 47% coverage was only 11%, while this condition created an acceptable acoustic solution (reverberation time) for both private and open plan offices.

6 Nomenclature

Symbol	Quantity	Unit
A	Area	m^2
c_{p_w}	Water specific heat capacity	$KJ \cdot kg^{-1} \cdot K^{-1}$

q	Heat transfer rate	W
q''	Heat flux (= q/A_{rad})	$W \cdot m^{-2}$
P	Power	W
$\dot{m}$	Water mass flow rate	$Kg \cdot s^{-1}$
U_{cc}	Cooling capacity coefficient	$W \cdot m^{-2} \cdot K^{-1}$
t	Temperature in ºC	°C
T	Temperature in K	K
t_a	Air temperature	°C
t_{op}	Operative temperature	°C
t_{mr}	Mean radiant temperature	°C
t_g	Globe temperature	°C
$t_{w,s}$	Water supply temperature	°C
$t_{w,r}$	Water return temperature	°C
$t_{w,m}$	Mean water temperature	°C
ΔT_w	Water temperature difference ($\Delta T_W = t_{w,r} - t_{w,s}$)	K
v	air velocity	$m \cdot s^{-1}$
$A_{absorption}$	Equivalent sound absorption area	Sabin, m^2
c	Speed of sound	$m \cdot s^{-1}$
d	Decay rate	$dB \cdot s^{-1}$
T_{60}	Reverberation time	s
V	Volume	m^3

7 Acknowledgment

This work was supported by the California Energy Commission (CEC) Electric Program Investment Charge (EPIC) (EPN-14-009) "Optimizing Radiant Systems for Energy Efficiency and Comfort" and in-kind contributions of laboratory facilities by E.H. Price, Winnipeg, MB, Canada and by Armstrong World Industries, Lancaster, PA, USA. The authors would like to thank Mike Koupriyanov, Harmanpreet Virk and Jared Young for their help in the laboratory testing.

8 References

[1] J. Babiak, B. W. Olesen, and D. Petras, *REHVA Guidebook No 7: Low Temperature Heating and High Temperature Cooling*, 1st ed. Belgium: Federation of European Heating and Air-conditioning Associations, 2009.

[2] R. A. Meierhans, "Slab cooling and earth coupling," *ASHRAE Trans.*, vol. 99, no. 2, pp. 511–520, 1993.

[3] H. E. Feustel and C. Stetiu, "Hydronic radiant cooling—preliminary assessment," *Energy Build.*, vol. 22, no. 3, pp. 193–205, 1995.

[4] B. W. Olesen, M. De Carli, M. Scarpa, and M. Koschenz, "Dynamic Evaluation of the Cooling Capacity of Thermo-Active Building Systems.," *ASHRAE Trans.*, vol. 112, no. 1, 2006.

[5] B. Lehmann, V. Dorer, and M. Koschenz, "Application range of thermally activated building systems tabs," *Energy Build.*, vol. 39, no. 5, pp. 593–598, 2007.

[6] M. Gwerder, B. Lehmann, J. Tödtli, V. Dorer, and F. Renggli, "Control of thermally-activated building systems (TABS)," *Appl. Energy*, vol. 85, no. 7, pp. 565–581, 2008.

[7] ASHRAE, *Handbook HVAC systems and equipment*. Atlanta, GA, USA: American Society of Heating, Refrigerating and Air-Conditioning Engineers, Inc., 2012.

[8] T. Moore, F. Bauman, and C. Huizenga, "Radiant cooling research scoping study," Center for the Built Environment, Berkeley, CA, USA, 2006.

[9] F. Bauman, T. Webster, H. Zhang, and E. Arens, "Advanced Design and Commissioning Tools for Energy-Efficient Building Technologies," Center for the Built Environment, 2012.

[10] D. Egan, *Architectural Acoustics*. Richmond, VA, USA: J. Ross Publishing Classics, 2007.

[11] P. Chigot, "Office buildings and natural cooling: room acoustic demands and influence of acoustic treatment on thermal performance," in *Proceedings of Inter-Noise 2010*, Lisbon, Portugal, 2010, pp. 13–16.

[12] P. Weitzmann, E. Pittarello, and B. W. Olesen, “The cooling capacity of the thermo active building system combined with acoustic ceiling,” in *Nordic Symposium on Building Physics 2008*, Copenhagen, Denmark, 2008.
[13] H. Peperkamp and M. Vercammen, “Thermally activated concrete slabs and suspended ceilings,” in *NAG-DAGA International Conference on Acoustics*, Rotterdam, Netherlands, 2009.
[14] Y. Le Muet, H. Peperkamp, and R. Machner, “Combining thermally activated cooling technology (TABS) and high acoustic demand: Acoustic and thermal results from field measurements,” in *Inter-Noise 2013*, Innsbruck, Austria, 2013.
[15] Ecophon, “Knowledge guide: Thermally activated building systems,” Saint-Gobain Ecophon AB, Yttervägen, Sweden, 2014.
[16] CEN, “14240, Ventilation for buildings - chilled ceiling testing and rating,” European Committee for Standardization, Brussels, Belgium, 2004.
[17] B. W. Olesen, E. Michel, F. Bonnefoi, and M. De Carli, “Heat exchange coefficient between floor surface and space by floor cooling-theory or a question of definition,” *ASHRAE Trans.*, vol. 106, no. 1, pp. 684–694, 2000.
[18] ISO, EN, “7726, Ergonomics of the Thermal Environment – Instruments for Measuring Physical Quantities,” International Standards Organization, Geneva, Switzerland, 2001.
[19] ISO, EN, “13005, Guide to the Expression of Uncertainty of Measurement,” International Standards Organization, Geneva, Switzerland, 2000.
[20] JCGM, “JCGM 100:2008, Evaluation of Measurement Data - Guide to the Expression of Uncertainty in Measurement (GUM 1995 with minor corrections),” Joint Committee for Guides in Metrology (JCGM), International Bureau of Weights and Measures (BIPM), Sèvres, France, 2008.
[21] ASTM, “Standard C423-09a, Standard Test Method for Sound Absorption and Sound Absorption Coefficients by the Reverberation Room Method,” American Society for Testing Materials (ASTM), West Conshohocken, Pennsylvania, USA, 2009.
[22] DIN, “18041:2004-05, Acoustical quality in small to medium-sized rooms,” German Institute for Standardization, Beuth Verlag GmbH, Berlin, Germany, 2004.
[23] M. Ermann, *Architectural acoustics illustrated*. Hoboken, NJ, USA: John Wiley & Sons, 2015.
[24] ASHRAE, *Performance Measurement Protocols: Best Practices Guide*. Atlanta, GA, USA: American Society of Heating, Refrigerating and Air-Conditioning Engineers, Inc., 2012.
[25] J. D. Feng, S. Schiavon, and F. Bauman, “Cooling load differences between radiant and air systems,” *Energy Build.*, vol. 65, pp. 310–321, 2013.
[26] H. B. Awbi, *Ventilation of buildings*. Abingdon, England: Taylor & Francis, 2003.
[27] A. Novoselac, B. J. Burley, and J. Srebric, “New convection correlations for cooled ceiling panels in room with mixed and stratified airflow,” *HVACR Res.*, vol. 12, no. 2, pp. 279–294, 2006.
[28] M. Frontczak, S. Schiavon, J. Goins, E. Arens, H. Zhang, and P. Wargocki, “Quantitative relationships between occupant satisfaction and satisfaction aspects of indoor environmental quality and building design,” *Indoor Air*, vol. 22, no. 2, pp. 119–131, 2012.
[29] J. Kim and R. de Dear, “Workspace satisfaction: The privacy-communication trade-off in open-plan offices,” *J. Environ. Psychol.*, vol. 36, pp. 18–26, 2013.